

Application of a minimal model to Kongsvegen and Kronebreen

Bachelor Thesis by Eef van Dongen
Supervised by dhr. prof. dr. J. Oerlemans,
Institute for Marine and Atmospheric Research Utrecht (IMAU)

January 8, 2014



Ground view of the calving front of Kongsvegen on 14. July 2009; seagulls are attracted by nutrients in the glacial runoff and rich marine life.^[1]

Abstract

The long-term behaviour of the Kongsvegen-Kronebreen system is studied with a minimal glacier model, based on heavily parameterized representations of the surface mass balance and calving flux. Kongsvegen is about 27 km long, surging glacier, coupled to the larger calving glacier Kronebreen of about 50 km. The model is driven by a climate reconstruction from 1300 AD onwards, based on ice-core data from Lomonosovfonna and climate records from Longyearbyen. The model is calibrated to match the systems observed length in 1936, before Kongsvegens last surge occurred. We find that the climate variations are not able to produce the retreat observed after the surge, and conclude that an increased calving flux accounts for the observed retreat.

If climatic conditions will remain as they were for the period 1990-2007, Kronebreen will reach a steady state around 2160, after it has lost 21% of its volume in 2005. For the RCP8.5 scenario by the IPCC, the equilibrium line will rise with 1.16 m yr^{-1} , resulting in an accelerated volume loss resulting in 41% loss in the year 2200 compared to 2005, and ultimately the glacier disappears several hundreds of years later.

Contents

1	Introduction	3
1.1	Calving glaciers	3
1.2	Surging glaciers	3
2	Study area: the Kronebreen-Kongsvegen system	4
2.1	Observed variations of the glacier front	4
3	The model	6
3.1	Calving law	7
3.2	Describing the surge	7
3.3	Solving the continuity equation	7
3.4	Interaction between Kronebreen and Kongsvegen	8
4	Calibration	8
5	Results	13
5.1	Simulation of the past	13
5.2	Relation between glacier length equilibrium-line altitude	15
5.3	Kronebreen and Kongsvegen in a warming climate	16
6	Discussion and conclusion	16
7	Acknowledgements	17
A	Derivations	19
A.1	Computation of mean bed elevation and slope	19
A.2	Evaluation of the continuity equation	20
B	Fortran code	22

1 Introduction

The fifth assessment report by the IPCC states that the average rate of ice loss from glaciers around the world, was very likely 226 Gt yr^{-1} over the period 1971 to 2009, and very likely 275 Gt yr^{-1} over the period 1993 to 2009.¹ Realizing that 100 Gt of ice loss is equivalent to about 0.28 mm yr of global mean sea level rise, stresses the importance of understanding the long-term behaviour of glaciers.

One way of obtaining a better understanding of the behaviour of glaciers is by modelling them, using physical relations that describe interactions between the glacier and its environment. The modelling of glaciers often requires large spatial numerical models. With constantly increasing computer power available, it is tempting to try to implement as many mechanisms in a model as possible. A disadvantage of this, is that it becomes almost impossible to be

able to understand such a comprehensive model entirely in the relatively short time available for this research. That is why we used a different approach in this study. The long-term behaviour of a glacier is determined by its mass budget, i.e. snowfall, melt and possibly loss of ice to the sea. These processes depend mainly on the climate and topographic characteristics of a glacier and less on the detailed ice mechanics. The model used in this study is kept as straightforward as possible, and focuses on the interaction between glaciers and climate. It has already been shown that this approach is a remarkably effective way to capture the long-term behaviour of a glacier, despite (or maybe even due to) its simplicity.^[13]

The model used is called a minimal model since it requires no spatial resolution. The theory of the model has been developed in *Minimal Glacier Models*^[12] and will be summarized in Section 3. It is an excellent model for this study since it is relatively easy to understand and also to adjust it to model different glaciers. This simple model is used as a learning tool, that is used to explore which characteristics of the glacier really matter in grasping the long-term behaviour of a glacier. Besides simulating the observed length of the glaciers, experiments are done to investigate what effect further climate warming will have on Kongsvegen and Kronebreen. The main goal of this paper is to explore the processes driving the glaciers. We aim to find out whether this is mainly the climate forcing, or that other aspects might be of greater importance.



Figure 1.0.1: Kronebreen with Colletthøgda in the background, 2009. Photo: M. Sund.

1.1 Calving glaciers

Glaciers ending in water lose ice by calving, over 60% of the glaciers in Svalbard terminate in tidewater and are therefore calving glaciers. The term tidewater glacier was introduced by Russell^[19] and defined as '*glaciers which enter the ocean and calve off to form bergs.*' The calving flux is estimated to account for 17-25% of the mass loss of calving glaciers.^[2] The details of the calving process are complicated and for that very reason it is interesting to investigate whether a simple model is able to simulate the behaviour of the two tidewater glaciers Kongsvegen and Kronebreen.

Several studies have shown that calving is a complex and diverse process, with a broad range of environmental controls. Calving permits much larger volumes of ice to be lost than would be possible through only surface melt. Factors that may affect the calving process include erosion caused by temperature changes at the glacier front and undersea calving of submarine platforms. In addition, bands of structural weakness along which fractures may propagate, as well as possibly present surface and bottom crevasses tend to control the rate of iceberg production to some extent.^[23]

1.2 Surging glaciers

A major part of the Svalbard glaciers are also found to be surge-type glaciers.^[21] A.S. Post^[18] defines a surging glacier as '*one which periodically (15-100+ years) discharges an ice reservoir by means of a sudden, brief, large-scale ice displacement, which moves 10 to 100 or more times faster than the glaciers normal flow*

¹Excluding glaciers on the periphery of the ice sheets.

rate between surges. Glacier surges are not unique events which might result from exceptional conditions such as earthquakes, avalanches, or local increases in snow accumulation. These movements are apparently due to some remarkable instability which occurs at periodic intervals in certain glaciers.' So during a surge, mass is suddenly transferred to lower regions of the glacier where melt rates are known to be higher. Surging glaciers typically undergo two alternating phases. The short surge phase of active rapid flow, usually lasting from one to three years, is followed by a much longer quiescence phase of slow flow lasting from ten to hundred years.^[9] The first attempt to model the behaviour of a surging glacier was done ten years later by W.F. Budd.^[3] Afterwards, more theories were developed in which the mechanisms behind the surge were investigated.^[7,4] The discussion mainly focuses on the relation between sliding, basal drag and hydraulics. In this study, we do not try to clarify the mechanisms behind the surge behaviour. We aim to investigate the effect of a surge on the length of a glacier, since Kongsvegen is of this type.

2 Study area: the Kronebreen-Kongsvegen system

Kongsvegen and Kronebreen are situated in north-west Spitsbergen, an island of Svalbard. Before describing the model used, a summary of the available information on the glaciers will be provided. Many measurements are done on both Kronebreen and Kongsvegen, since they are located close to the weather station Ny-Ålesund as seen on Figure 1.2.1. This makes the glaciers interesting for an investigation on the impact of climate change on glaciers. The glaciers have a joint calving front in the Kongsfjorden. Kongsvegen is about 27 km long, with elevations up to 800 m a.s.l. It covers a total area of approximately 180 km². The glacier has been in a quiescent phase since its last surge which was observed in 1948.^[8] Kronebreen is some 50 km long, spanning elevations of 0-1400 m above sea level. Its area is circa 390 km², when the contributory glacier Infantfonna is taken into account as well.^[11] Great differences exist in the dynamics of the two glaciers. Kongsvegen has very low velocities now it is in its quiescent phase, a maximum of 4 m yr⁻¹ was measured at the equilibrium line.^[8] Observed average annual velocities for Kronebreen vary from 300 to 800 m yr⁻¹ at the front.^[6] Such high velocities are consistent for measurements made in 1964, 1986 and around 2000-2002.^[11] Kronebreen is therefore counted among the most persistent fast-flowing glaciers in Svalbard which causes its heavily crevassed surface, as seen in Figure 1.0.1. This high velocity is caused by its large accumulation area which is squeezed through a narrowing just before its confluence with Kongsvegen, as shown in Figure 1.2.1. Kongsvegens confluence with Kronebreen is about 5 km from the calving front. Currently, Kongsvegen has almost effectively retreated onto land.

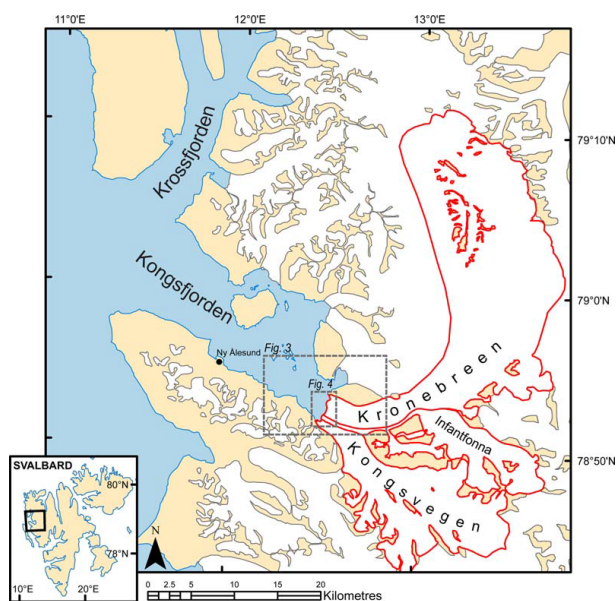


Figure 1.2.1: Regional setting of Kongsfjorden and the glaciers of this study, Kronebreen and Kongsvegen as well as another glacier called Infantfonna. Location of the large map is shown with respect to the islands of Svalbard in the lower left corner. Location of Ny-Ålesund is indicated.^[22]

2.1 Observed variations of the glacier front

Front positions were measured from 1923 and an overview of these observations is given by Sund et al.^[20] A large retreat of up to 1.4 km occurred between 1923 and 1924 (Figure 2.1.1a). The area of retreat corresponds with an area of larger water depth, as seen in Figure 2.1.1b. Both before and after the surge in 1948, the glacier front of the Kronebreen-Kongsvegen system was situated in the area between the 1924 and 1970 positions. In 1936 the width of Infantfonna and Kongsvegen was almost equal and together constituted ~ 25% of the total width of the ice cliff dominated by Kronebreen. Kongsvegen contributed to increased ice thicknesses in the terminal part of Kronebreen during the surge, as Kongsvegen occupied about half of the ice cliff width by then. After Kongsvegens surge of 1948, the Kronebreen-Kongsvegen system has been observed to undergo progressive thinning and glacier front retreat. During 22 years after the surge the retreat rate is 45 112 m

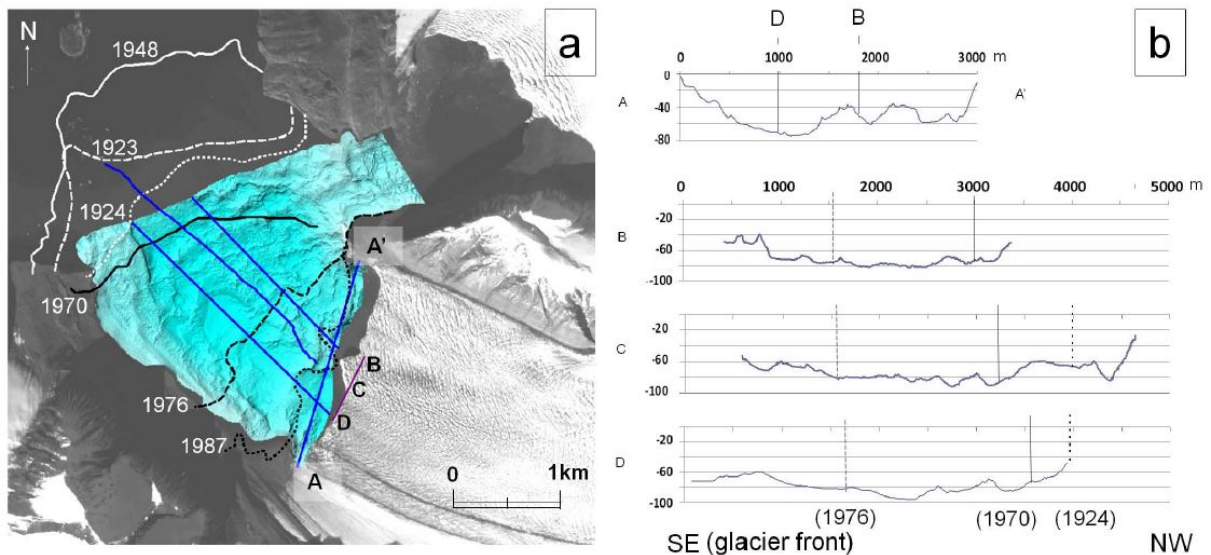


Figure 2.1.1: (a) Shaded bathymetry relief (Norwegian Mapping Authority, Norwegian Hydrographic Service) and profile tracks (A-D), with front positions. Background image: SPOT 5. (b) Transversal profile (A-A') with positions of profiles B and D indicated. Bed profiles are shown from southeast towards northwest (B-D). Profile C is from 200 kHz echo sounding, the others are derived by Norwegian Mapping Authority. Distances are measured from purple line along front in (a). Vertical lines indicate front positions in years corresponding to line legend in (a).^[20]

yr^{-1} , as the glacier retreats into gradually deeper water. By 1964, Kongvegen was being pushed back towards south, Infantfonna was no longer extending all the way to the sea and Kronebreen covered 65% of the width. The most rapid period of retreat occurred between 1970 and 1976, when the southern part of the ice cliff retreated by $\sim 2 \text{ km}$ (333 m yr^{-1}). This seems to coincide with a depression in the sea floor in this area, as is shown in Figure 2.1.1b. The following eleven years until 1987, the retreat rate is up to 120 m yr^{-1} .

Long-term patterns of elevation change on the lower tongue of Kronebreen were determined by comparing digital terrain models (DTMs) for 1964 and 2007. All parts of the lower tongue of the glacier have lowered between 1964 and 2007, with the greatest amount of lowering occurring in the south, in the area formerly occupied by Kongsvegen. The surface melt at the stake ($\sim 110 \text{ m a.s.l.}$) showed melt of $\sim 3 \text{ m}$ water equivalent (w eq.) during summer 2008 (30 May-28 September). By 2007, the partition between the three streams was almost back to the 1936 situation as Kronebreen occupied $\sim 70\%$ of the width.

Glacier front positions for selected years between 1987 and 2008 are shown in Figure 2.1.2. Most parts of the glacier front experienced net retreat over this period. The greatest amount of net retreat occurred on the northern side of Kronebreen, which retreated up to 330 m ($\sim 20 \text{ m yr}^{-1}$) between 1990 and 2007. Further south towards Kongsvegen, a net retreat of circa 200 m has been observed in the same period. The 1998 ice-front position lies up to 200 m west of the 1990 position, suggesting a slight advance of the glacier during the 1990s. It should be noted that the positions for 1987, 1990 and 1998 (Figure 2.1.2) are taken from single-day pictures, all acquired in summer. Major calving events might have occurred shortly before or after images were acquired. The water depth at the calving front is $\sim 60 \text{ m}$. The front

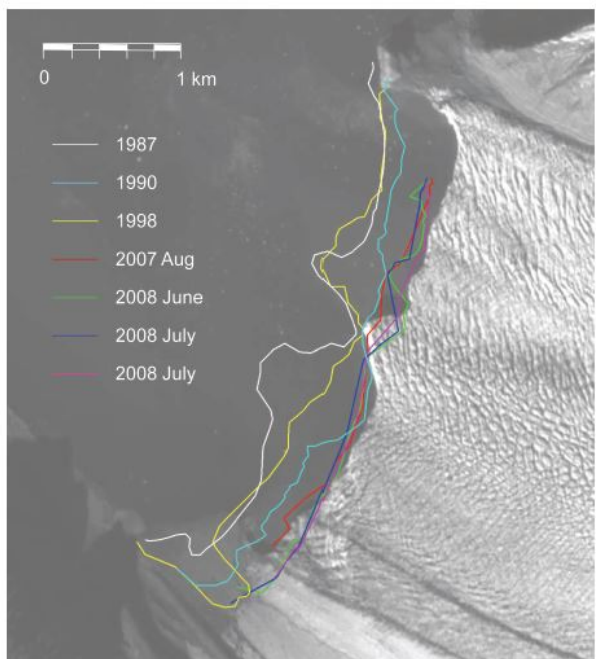


Figure 2.1.2: Glacier front fluctuations between 1987 and 2008. Background image: SPOT 5. Maximum retreat for certain position along the front during this period is $\sim 700 \text{ m}$ and minimum is $\sim 50 \text{ m}$. The 1987, 1990 and 1998 positions are drawn from NPI maps Kongsfjorden (1990 and 2000 editions), 2007 and 2008 lines are from stereo photogrammetry.^[20]

of Kongsvegen, squeezed by the more dynamic glacier Kronebreen, has almost effectively retreated on land. The observations seem to indicate that the front position for Kronebreen has stabilized. In this study, we will investigate how stable this position really is and how sensitive it is to perturbations.

3 The model

The model uses no spatial resolution, because integration is done over the entire glacier area along the flow line such that it is possible to derive an explicit expression for $\frac{dL}{dt}$. The evolution of the glacier is calculated from an integrated continuity equation, where the rate of change in the volume is assumed to be equal to the surface mass balance (B_s) and ice loss at the glacier front (F), such that

$$\frac{dV}{dt} = B_s + F, \text{ where } B_s \text{ is defined as } \int \dot{b} dx dy. \quad (3.0.1)$$

In this equation, V is ice volume, t is time and \dot{b} is the balance rate. The x -coordinate is defined along the flowline of the glacier, from zero at the top to L at the glacier front. The y -coordinate represents the width of the glacier at a certain position along the flowline. The balance rate \dot{b} is defined as the net annual gain or loss of mass at the glacier surface.^[14] A glacier consists of an accumulation zone where \dot{b} is positive and an ablation zone where \dot{b} is negative, hence mass melted over the summer is not entirely compensated by snowfall during the winter in the latter case. The two zones are separated by a mainly theoretically defined line called the equilibrium line, where \dot{b} is zero. Generally speaking, the accumulation zone is the upper part of the glacier because \dot{b} increases with altitude. There are mainly two reasons why this is the case. The most evident one is that air temperature decreases about six to seven degrees Kelvin per meter. Besides that, precipitation commonly increases with altitude. The precipitation on higher parts of mountains can be twice as large as in the valleys.^[12] As will be explained in Section 4, it is reasonable to approximate the function $\dot{b}(z)$ with a linear function such that

$$\dot{b}(z) = \beta(z - E). \quad (3.0.2)$$

Here β is defined as $\frac{d\dot{b}}{dz}$, E is the altitude of the equilibrium line and z represents the surface elevation. The model assumes a constant width $W(x)=W$ for the glacier. This assumption might seem crude but it will be justified in Section 4. Due to this assumption, \dot{b} only depends on the x -coordinate such that

$$B_s = \int \dot{b} dx dy = W \int_0^L \dot{b} dx = W\beta \int_0^L (z(x) - E) dx, \quad \text{where } z(x) = b(x) + H(x). \quad (3.0.3)$$

Here b is the bed elevation and H is the ice thickness. Using the mean bed elevation and mean ice thickness, defined as

$$\bar{b} = \frac{1}{L} \int_0^L b(x) dx \quad \text{and} \quad H_m = \frac{1}{L} \int_0^L H(x) dx, \quad (3.0.4)$$

an expression for B_s can be obtained. Substituting eq. 3.0.4 into eq. 3.0.3 gives

$$B_s = W\beta(\bar{b} + H_m - E)L. \quad (3.0.5)$$

In this case the bed elevation is parameterized using Gaussian and exponential functions combined with a linear component such that

$$b(x) = b_0 e^{-\frac{x}{x_2}} + b_1 e^{-\left(\frac{x-x_0}{x_l}\right)^2} - sx. \quad (3.0.6)$$

The expression for \bar{b} is derived in Appendix A.1. A meaningful expression for H_m is derived from runs in numerical model studies based on the shallow ice approximation, to be

$$H_m = \frac{\alpha_m}{(1 + \nu \bar{s})} \sqrt{L}. \quad (3.0.7)$$

Here α_m and ν are constants. \bar{s} is the mean slope of the bed, which is derived for the used bed profile given by eq. 3.0.6. The derivation can be found in Appendix A.1.

3.1 Calving law

A strong correlation between calving rates and water depth has been confirmed for several tidewater glaciers and it has also been shown before that the calving rate is indeed proportional to the water depth at the terminus.^[9] The calving rate is assumed to be linearly proportional to the water depth d at the glacier front and to depend on the cross-sectional area of the calving front. Therefore, the calving flux is defined as

$$F = -cdH_fW, \quad (3.1.1)$$

where H_f is the ice thickness at the glacier front and c is called the calving constant. The ice thickness at the front is assumed to be a fraction κ of the mean ice thickness.^[12] The expression of eq. 3.1.1 will only be meaningful if the ice thickness H_f is large enough to keep the glacier from floating at the front, i.e.

$$H_f > \frac{\rho_w}{\rho_i}d = \delta d, \quad (3.1.2)$$

where δ is the fraction of water to ice density, such that δd is the ice thickness at which the glacier front just starts to float. Hence

$$H_f = \max(\kappa H_m, \delta d). \quad (3.1.3)$$

3.2 Describing the surge

For imposing the surge, a new parameter S is introduced in the expression of the mean ice thickness, accordingly

$$H_m = S(t) \frac{\alpha_m}{(1 + \nu \bar{s})} \sqrt{L}. \quad (3.2.1)$$

In the 'normal mode', representing a glacier without surging behaviour or a glacier in its quiescent phase, $S=1$. A surge is initiated by a sudden decrease in the value of S . The sudden thinning of the glacier results in a rapid increase of the glacier length due to the conservation of volume. A surge is imposed to the model by prescribing

$$S(t) = 1 - S_0(t - t_0)e^{-\left(\frac{t-t_0}{t_s}\right)^2}, \quad (3.2.2)$$

as in *Minimal Glacier Models*.^[12] The surge starts when $t = t_0$, S_0 determines the amplitude of the decrease in H_m and t_s describes the length of the surge phase. As will turn out in the next section, it is useful to calculate the derivative with respect to t . Using elementary differentiation rules gives

$$\frac{dS}{dt} = S_0 \left(\frac{t - t_0}{t_s} - 1 \right) e^{-\left(\frac{t-t_0}{t_s}\right)^2} \quad (3.2.3)$$

3.3 Solving the continuity equation

Since all parameters in the continuity equation are defined, it is now possible to derive an expression for $\frac{dL}{dt}$ analytically. Using $V = WH_mL$, and the product and chain rule for differentiation results in

$$\begin{aligned} \frac{dV}{dt} &= \frac{d}{dt} (WH_mL) \\ &= W \left(\frac{dL}{dt} \left[\frac{3}{2}H_m - \frac{L\nu H_m}{(1 + \nu \bar{s})} \frac{\partial \bar{s}}{\partial L} \right] + \frac{H_mL}{S(t)} \frac{dS}{dt} \right), \end{aligned}$$

as derived in Appendix A.2. Together with substitution of eq. 3.0.5 and eq. 3.1.1 into eq. 3.0.1 yields

$$\frac{dL}{dt} = \left(\frac{B_s + F}{W} - \frac{H_mL}{S(t)} \frac{dS}{dt} \right) \Psi^{-1} \text{ where } \Psi = \left[\frac{3}{2}H_m - \frac{L\nu H_m}{(1 + \nu \bar{s})} \frac{\partial \bar{s}}{\partial L} \right], \quad (3.3.1)$$

as described in Appendix A.2. The expression for $\frac{\partial \bar{s}}{\partial L}$ is derived in Appendix A.1, which completes the expression for $\frac{dL}{dt}$. This differential equation is solved using the simple Euler forward method. This method uses the first degree Taylor series of a function f at t , such that

$$f(t + \Delta t) = f(t) + \Delta t f'(t) + \frac{\Delta t^2}{2} f''(\xi) \text{ where } \xi \in [t, t + \Delta t]$$

Now $\frac{\Delta t^2}{2} L''(\xi)$ is assumed to be approximately zero for small Δt , so L is calculated using

$$L(t + \Delta t) \approx L(t) + \Delta t \frac{dL}{dt}. \quad (3.3.2)$$

In the subsequent calculations, we use $\Delta t = 1/8$.

3.4 Interaction between Kronebreen and Kongsvegen

A great deal of the long-term behaviour of the glacier front seems to be caused by the interaction of Kongsvegen and Kronebreen. The glaciers confluence at ~ 3 km from their current calving front. Since a way to model two parallel positioned, interacting glaciers has not yet been developed, a similar approach will be used as was done in *Minimal Glacier Models* for the Vadret da Morteratsch system.^[12] The Kronebreen-Kongsvegen system will be considered as a two-component system. Kongsvegen will be defined to have a maximum length $L_{kv,max}$ of 22.1 km, as in Figure 3.4.1. When $L_{kv,max}$ is reached, its total surface mass balance or advance due to surging, will be added to the mass balance for Kronebreen. This results in (with kv as index for Kongsvegen and kb for Kronebreen) two possible situations, if $L_{kv} < L_{kv,max}$:

$$\frac{dL_{kb}}{dt} = \left(\frac{B_{s,kb} + F}{W_{kb}} \right) \Psi_{kb}^{-1}; \quad \frac{dL_{kv}}{dt} = \left(\frac{B_{s,kv}}{W_{kv}} - \frac{H_{m,kv} L_{kv}}{S(t)} \frac{dS}{dt} \right) \Psi_{kv}^{-1} \quad (3.4.1)$$

If on the other hand $L_{kv} = L_{kv,max}$ and $\frac{dL_{kv}}{dt}$ as defined above is positive, then:

$$\frac{dL_{kb}}{dt} = \left(\frac{B_{s,kb} + F}{W_{kb}} + \frac{B_{s,kv}}{W_{kb}} - \frac{H_{m,kv} L_{kv} W_{kv}}{W_{kb}} \frac{dS}{dt} \right) \Psi_{kb}^{-1}; \quad \frac{dL_{kv}}{dt} = 0. \quad (3.4.2)$$

The second requirement (of $\frac{dL_{kv}}{dt}$ being positive) stems from the consequence that it will immediately cause Kongsvegen retreat from its maximum length, so the glaciers will be decoupled. The derivation of eq.3.4.2 is written in Appendix A.2 as well.

4 Calibration

Kronebreen's bed topography was recently mapped. Radar data were obtained in 2009 and 2010 using 10 Mhz radar flown by helicopter over the glacier. Other data sets were combined with the radar data to create a comprehensive digital elevation model of both the fjord and glacier. Bathymetry for most of Kongsfjord was compiled from older sources. Bathymetry toward the present Kronebreen terminus was obtained from swath bathymetry obtained by University of Tromsø and the Norwegian Mapping Authority.

An article by Soviet scientists Y. Macheret and Y. Zhuravlev in 1982 was a first report on Kongsvegen's bed topography. Since then aerial soundings have been carried out by different institutes and scientists. These measurements are brought together in an article published in 1991^[5], which we used to digitalize the bed profile. The surface elevation is taken from maps by the Norwegian Polar Institute.^[10] The combined bed and elevation profiles can be found in Figure 4.0.2. With this information at hand, α_m can be calculated using eq. 3.0.7, hence $\alpha_m = \frac{H_m(1+\nu\bar{s})}{\sqrt{L}}$. This results in $\alpha_{m,kb} = 1.43 \text{ m}^{1/2}$ and $\alpha_{m,kv} = 2.27 \text{ m}^{1/2}$ where H_m and \bar{s} are calculated from Figure 4.0.2, giving $H_m = 286.1 \text{ m}$ and $\bar{s} = 0.023$ for Kongsvegen and $H_m = 250.2 \text{ m}$ and $\bar{s} = 0.025$ for Kronebreen. The difference between these two values of α_m is a result of the differences in the glaciers dynamics. Kronebreen flows about a hundred times faster than Kongsvegen, therefore mass is constantly transferred to lower regions. That is why Kronebreen turns out to be a relatively thin glacier. The value of ν is assumed to be equal to 10, as derived for the glacier Hansbreen in *Minimal Glacier Models* (p.70).^[12]

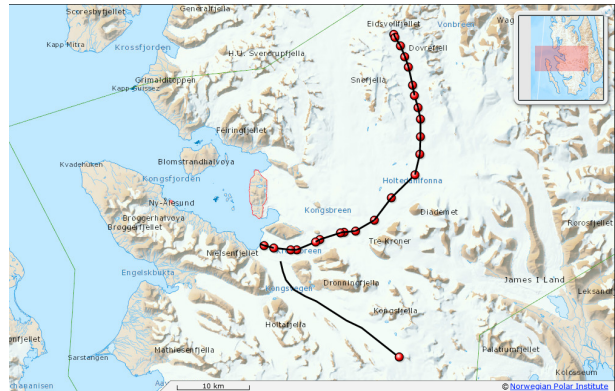


Figure 3.4.1: Flowlines of Kronebreen and Kongsvegen, with Kongsvegen defined to have a maximum length of 22.1 km at its confluence with Kronebreen.

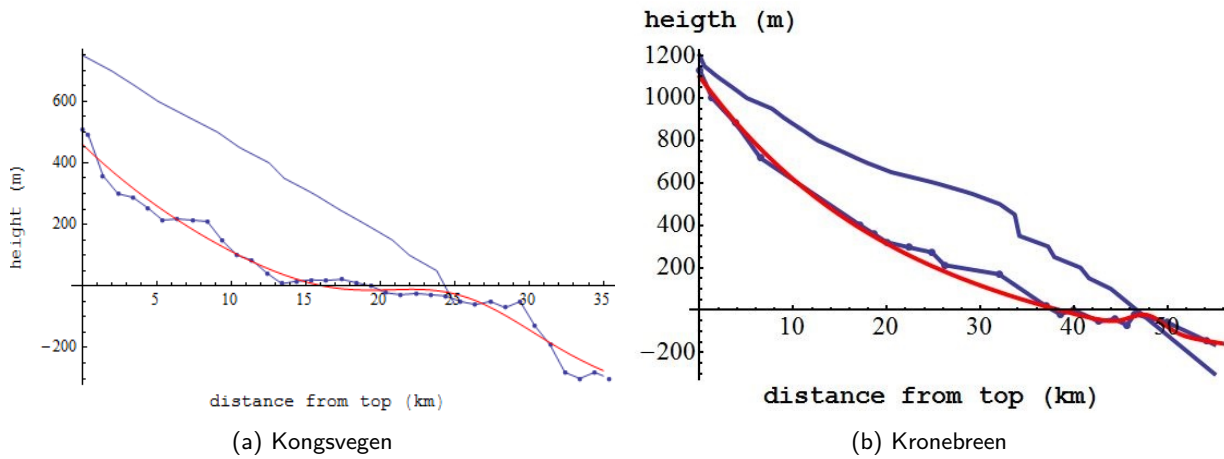


Figure 4.0.2: Measured basal and surface topography for both glaciers in blue. Parameterized bed profile as in eq. 3.0.6 in red.

The mean balance profile is approximated as a linear function of height, as in eq. 3.0.2. Using Figure 4.0.3 gives respectively $\beta = 0.0047 \text{ m w.e. m}^{-1}$ and $\beta = 0.0049 \text{ m w.e. m}^{-1}$ for Kongsvegen in the periods 1969-95 and 1995-2007. $\beta = 0.0051 \text{ m w.e. m}^{-1}$ and $\beta = 0.0052 \text{ m w.e. m}^{-1}$ were measured for Kronebreen in the periods 1969-90 and 1990-2007. The average value of $0.0048 \text{ m w.e. m}^{-1}$ is converted to $\beta = 0.0053 \text{ m ice equivalent m}^{-1}$ to describe the balance rate. This overestimates the balance rate for the upper part of especially Kronebreen, but this effect is compensated by taking a constant width, since it is clear that the width increases with height for Kronebreen (see Figure 1.2.1).

Following Nuth et al^[11] a difference in the equilibrium line altitude is used for the glaciers, resulting in a 200 m higher E for Kronebreen compared to Kongsvegen. Since the glaciers are located close together, it is not likely that this difference will be caused by a difference in temperature. The difference will probably be a consequence of a difference in the amount of accumulation for both glaciers. Using the interactive map by the Norwegian Polar Institute^[10] $L_{kv,max}$ is defined to be 22.1 km. The same map is used to measure the width of the glaciers, 3.32 km for Kongsvegen and 3.11 km for Kronebreen were measured. This difference is not significant (especially when realizing that the width is approximated already by assuming it to be constant), hence it is not taken into account when linking their mass balances. This leads to a less complicated equation for $\frac{dL_{kb}}{dt}$, as shown in A.2.5. In parameterizing the bed profiles we will not take every bump into account, because this will make it unnecessarily difficult to derive an expression for the mean slope. Therefore, only the overdeepening near the current front position is taken into account for both glaciers, as is shown in Figure 4.0.2. A bed topography that can be handled by the model is given in eq. 3.0.6. For Kongsvegen we derived $b_0 = 461.5 \text{ m}$, $x_2 = 12303 \text{ m}$, $s = 0.0092$, $b_1 = 146.8 \text{ m}$, $x_0 = 25421 \text{ m}$ and $x_l = -7088 \text{ m}$. These values are found using a least square fit where every parameter is adjusted one by one, with in size decreasing perturbations, until the sum

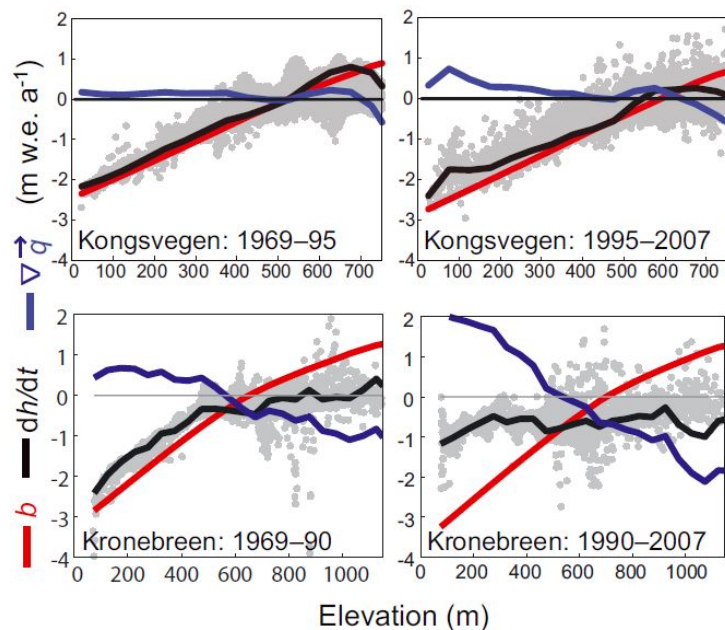


Figure 4.0.3: Annual average surface mass-balance rates b (red), elevation change rates $\frac{dh}{dt}$ (black) and the difference between them (blue) on Kongsvegen and Kronebreen. This difference has been shown to be zero on Kongsvegen^[8] hence this blue line actually represents an error term there. Measured elevation change rates are shown as gray pixels.

only the overdeepening near the current front position is taken into account for both glaciers, as is shown in Figure 4.0.2. A bed topography that can be handled by the model is given in eq. 3.0.6. For Kongsvegen we derived $b_0 = 461.5 \text{ m}$, $x_2 = 12303 \text{ m}$, $s = 0.0092$, $b_1 = 146.8 \text{ m}$, $x_0 = 25421 \text{ m}$ and $x_l = -7088 \text{ m}$. These values are found using a least square fit where every parameter is adjusted one by one, with in size decreasing perturbations, until the sum

of the squared differences $\sum(b(x_i) - b_i)^2$ was at a minimum. In this expression the x_i 's represent different positions for which the altitude of the bed b_i is known. Since this method does not guarantee that the minimum is global, different starting values were taken, all leading to the same values. A different approach is used for Kronebreen, since we want only the overdeepening near the glacier front to be taken into account. Therefore, the parameters were changed manually, until the overdeepening near the front was presented well. This resulted in the values $b_0 = 1089$ m, $x_2 = 25800$ m, $s = 0.00582$, $b_1 = 71.0$ m, $x_0 = 47800$ m and $x_l = 2550$ m. The value 0.4 will be assumed for κ , as was used for Hansbreen.¹³ This leaves only the calving constant, the equilibrium-line altitude and the prescription of the surge undefined. The length as observed in 1936, before the most recent surge occurred, is used to determine the calving constant c and the mean equilibrium-line altitude E_{gem} for the build-up period of the glacier. An experiment is carried out in which E_{kb} changes periodically from 1100 m to 500 m and back again using

$$E = E_0 + A_E \sin(2\pi t / P_E). \quad (4.0.3)$$

The period P_E in which E changes is taken to be 100 kyr, to make sure that the system is near to an equilibrium state. For some regions of E , the model shows hysteresis and does not have a steady state, as will be explained in Section 5.2. A steady state is never actually reached by a glacier in nature, especially not by a surging glacier. Nonetheless, it is useful to have a steady state as a reference, because it reveals basic properties of the glacier model. The experiment is done for three different values of the calving flux, with $A_E = 300$ m and $E_0 = 800$ m. In Figure 4.0.6, the modeled length is shown against the equilibrium line altitude of Kronebreen. The calibration length $L_{1936} = 51.5$ km, as derived from aerial photography^[22], is shown as well. Besides that, the modeled length of Kongsvegen is also shown. The length for Kongsvegen is the same for every value of c since we defined that Kronebreen is responsible for all calving. The length of Kongsvegen does depend on the height of the equilibrium line, and from Figure 4.0.6 it is clear that the glaciers will be linked only when $E_{\text{kb}} \leq 570$. Therefore a high enough c has to be taken, leading to a lower E_{gem} which will ensure that the glaciers are linked and that we will be able to investigate the influence of Kongsvegens surge on Kronebreen. A higher calving constant than 2 m yr^{-1} is tried as well but led to a maximum length which was too low to reach L_{1936} within the chosen domain of E . This domain was defined by requiring that the initial value of E is above the highest point of the bed. Besides that, an equilibrium-line altitude lower than 500 m does not seem reasonable anymore because a 200 m higher E has been reported in different studies.^[11,8] Note that the relation between E and L is nonlinear. For certain values of E , multiple steady states resulting in different glacier lengths are possible, depending on whether the glacier is advancing or retreating. This phenomenon will be discussed more detailed in Section 5.2. As derived from Figure 4.0.6, in a steady state where $c = 1.3 \text{ yr}^{-1}$ and $E_{\text{gem,kb}} = 507.5$ m, the length of Kronebreen will be equal to L_{1936} . For this reason, these values will be used as a starting point in the subsequent experiments.

The calving flux has been estimated for Kronebreen during two epochs, 1966-1990 (I) and 1990-2007(II). This was done by calculating the residual between the observed total mass balance and a modeled surface mass balance, based on observations of precipitation and temperature at Ny-Ålesund.^[11] The long-term calving flux is estimated to be $-0.14 \pm 0.03 \text{ km}^3 \text{ w.e. yr}^{-1}$ during epoch I, $-0.20 \pm 0.05 \text{ km}^3 \text{ w.e. yr}^{-1}$. The input of the model needs to be in m^3 ice equivalent, so taking the conversion factor $\delta = \frac{\rho_w}{\rho_i} \approx 1.1$ into account this yields

$$F_I = -0.14 \cdot 10^9 \cdot 1.1 = -1.54 \cdot 10^9 \text{ m}^3 \text{ i.e. yr}^{-1} \text{ and } F_{II} = -0.20 \cdot 10^9 \cdot 1.1 = -2.2 \cdot 10^9 \text{ m}^3 \text{ i.e. yr}^{-1}.$$

Using that $H_m = 250.2$ m, the water depth at the front is 60 m (see Section 2) and the width at the front is 3600 m (as measured using the map by NPI^[10]) gives with eq. 3.1.1 that

$$c = \frac{F}{-d\kappa H_m W} \text{ hence } c_I = 7.13 \text{ yr}^{-1} \text{ and } c_{II} = 10.19 \text{ yr}^{-1}. \quad (4.0.4)$$

These values for c are much higher than derived for the build-up period. A possible explanation could be that the calving flux is different for a advancing or retreating glacier, or maybe other processes, for example the ones named in the introduction, might have caused an increase in calving flux during these epochs. The effect of increasing the calving flux to the observed magnitude will be investigated later on.

Finally, a climatic forcing is introduced by varying E according to a derivation by Van Pelt et al.^[15] Here, changes in precipitation rates and temperature are translated to changes in E using

$$E(t) = E_0 + \frac{\partial E}{\partial T} T'(t) + \frac{\partial E}{\partial P} P'(t), \text{ and we use their values } \frac{\partial E}{\partial T} = 35 \text{ m K}^{-1}; \frac{\partial E}{\partial P} = -2.25 \text{ m \%}^{-1}, \quad (4.0.5)$$

as determined for Nordenskiöldbreen. Input data concerning P and T for calculating E' is taken from a climate reconstruction back to 1300 AD based on ice-core data from Lomonosovfonna as well as climate

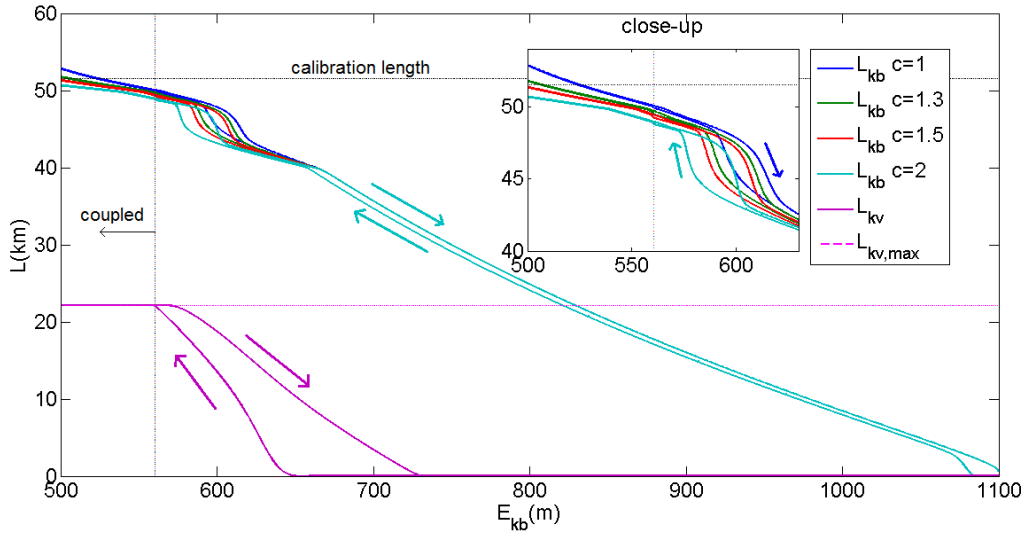


Figure 4.0.6: Glacier length of Kongsvegen and Kronebreen calculated with the minimal model as response to very slow forcing. Arrows indicate the paths of the hystereses. The value of E that ensures coupling, Kongsvegens maximum length and the calibration length of the year 1936 are indicated as well.

records from Longyearbyen, resulting in a prescription of E as shown in Figure 4.0.4.^[16] It should be noted that the average value of $E'(t)$ is not zero because E' is defined with respect to the period 1989-2010. The resulting average value of E' is -88 m, hence $E_0 = E_{gem} + 88$.

Now the only parameters that have not been defined are concerning the surge. The amplitude of the surge, S_0 , is defined by using the observation that the glacier advanced for 1.5 km.^[20] t_0 is determined by the observation that the glacier reached it maximum length in 1948. Therefore the surge is defined to start in 1947, its duration is defined by $t_s=2.5$ yr and $S_0=0.2$ yr⁻¹ turns out to lead to an advance of 1.5 km. Now all variables are defined and we are ready to do several climate experiments.

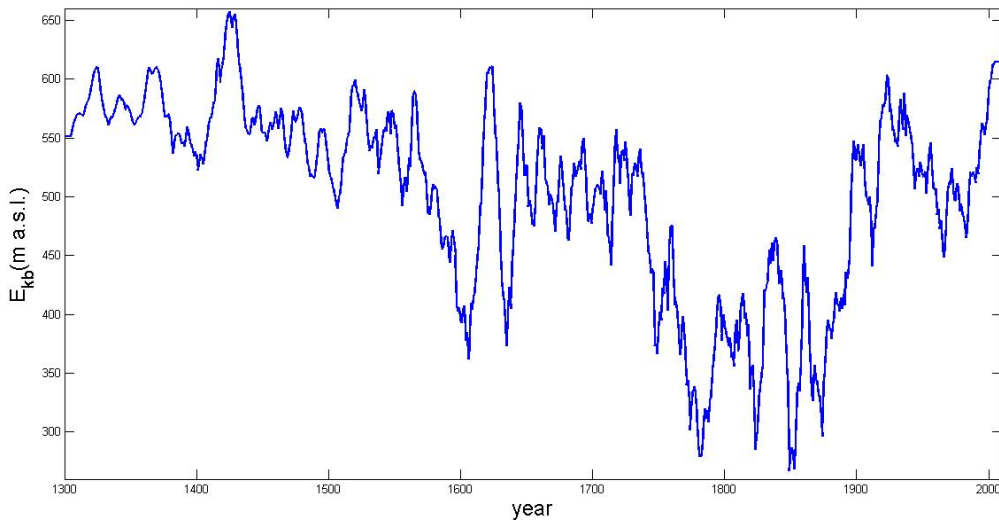


Figure 4.0.4: Climate forcing as derived by Van Pelt et al^[16], used to simulate the evolution of Kongsvegen and Kronebreen with $E_0 = 595.5$ m

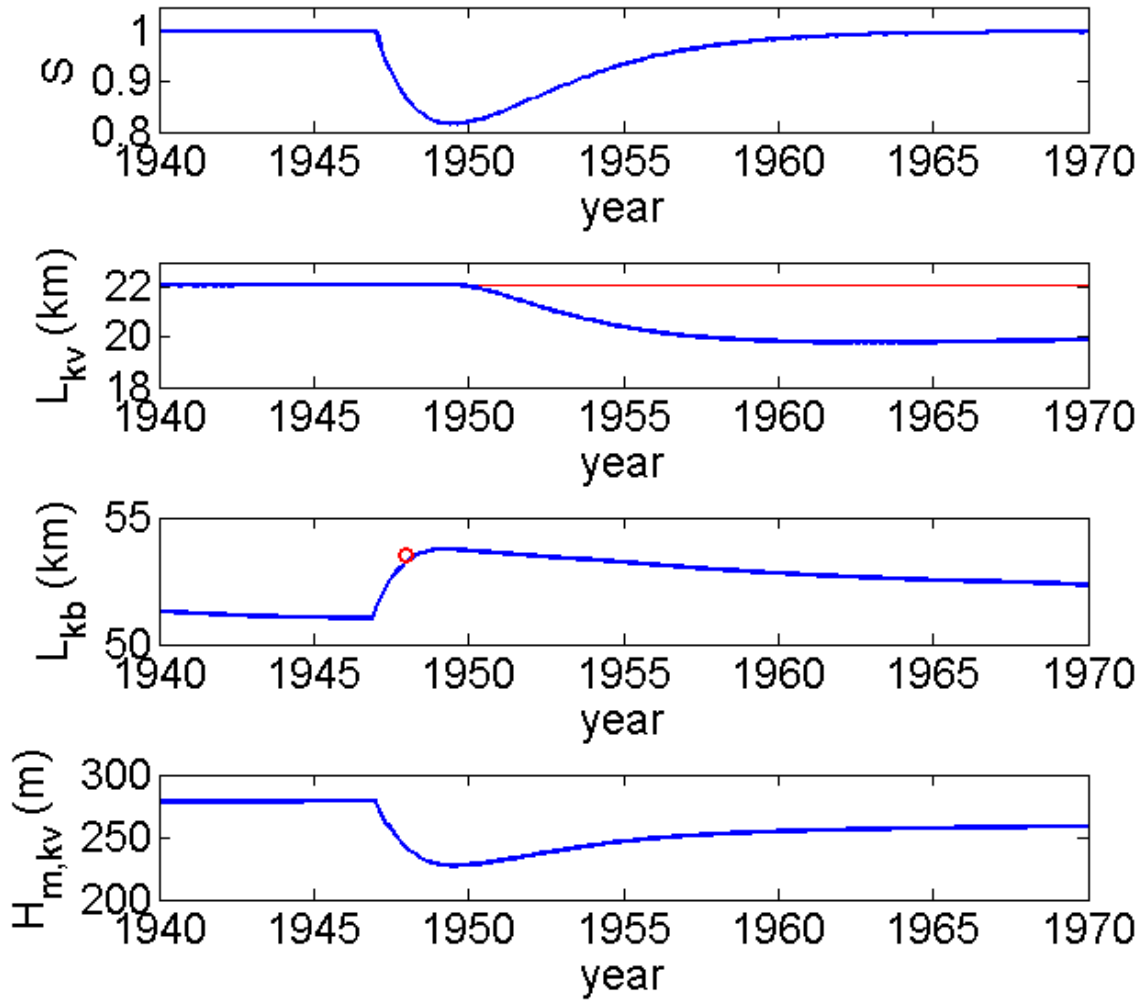


Figure 4.0.5: Surge event as imposed to the model by eq. 3.2.2. Maximum length of Kongsvegen in red and observed position of the joined front indicated with a red dot for L_{kb} . Note that Kongsvegen is already at its maximum length in 1947, therefore all advance due to its surge feeds Kronebreen.

5 Results

5.1 Simulation of the past

With all settings as explained in Section 4, a code is written in Fortran to solve the differential equations for the glacier lengths, as shown Appendix B. Since the system is not in a steady state in 1936, our reference state does not immediately lead to a match between the modeled and observed length in 1936. Therefore, the calving constant c is raised until this is the case, resulting in $c = 1.65 \text{ yr}^{-1}$. This leads to a build-up of the glaciers as shown in 5.1.1. The calving flux F has been divided by the glacier area (WL_{kb}) to obtain a number that has the same unit as the surface mass balance. A close-up of the period with observations available is shown in Figure 5.1.3. The simulated glacier length does not show the fast retreat that has been observed. Because it is not very obvious from the figure when the two glacier are linked, an extra parameter 'coupling' is included. This parameter is equal to one when the glaciers are linked and zero otherwise. When the glaciers are linked, the surface balance of Kongsvegen is divided by WL_{kb} to make it possible to compare its magnitude to the net and surface balance of Kronebreen.

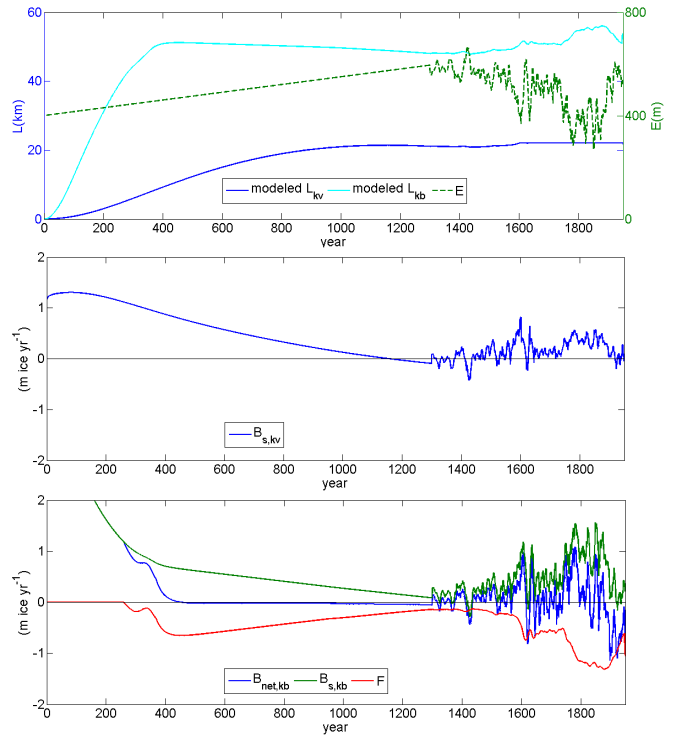


Figure 5.1.1: Build-up of the glacier system by increasing E from 357.5 m to $E_{gem} = 507.5 \text{ m}$, $c = 1.65 \text{ yr}^{-1}$, $\beta = 0.0053 \text{ m w.e. m}^{-1}$, $\alpha_{m,kb} = 1.43$, $\alpha_{m,kv} = 2.27$.

The behaviour of the Kronebreen-Kongsvegen system clearly cannot be explained only by the climate forcing. The model does not include overdeepenings in the bed profile for lengths observed in the period until now, though Nuth et al^[11] suggest that depressions in the bed might have caused the observed retreat. Trying to implement a more precise bed profile will make the continuity equation a lot more complex to solve. But since the calving flux has been estimated for two epochs, it is possible to adjust the calving constant to match the observed calving flux, without making the bed profile more complex.

Therefore, we will investigate what effect variation of the calving constant c with respect to time has on the correspondence of the observations and the model. As a result, we will rename c to be the calving parameter $c(t)$ from now on. Gaussian functions are added to the calving constant c_0 to model the estimated magnitude of the calving flux, such that

$$c(t) = c_0 + c_1 e^{-\left(\frac{t-p_1}{a_1}\right)^2} + c_2 e^{-\left(\frac{t-p_2}{a_2}\right)^2}. \quad (5.1.1)$$

Here the p_i 's define the year around which the increase is centered and the a_i 's define the length of the period of increase. The default value of $c(t)$ is $c_0 = 1.65 \text{ yr}^{-1}$, the other constants are chosen such that the mean of $c(t)$ over the two epochs matches the observed magnitude (eq.4.0.4). This results in a time dependence of the calving parameter as shown in Figure 5.1.2.

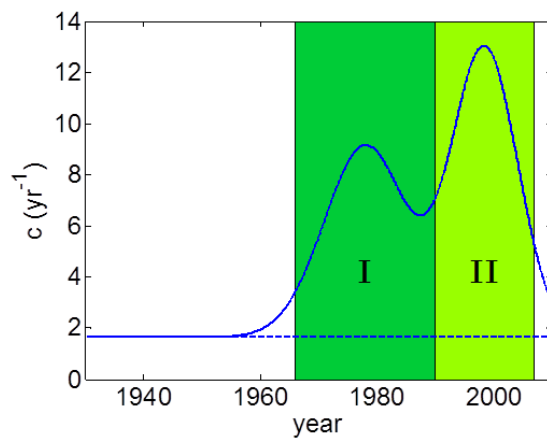


Figure 5.1.2: The time dependence of c as in eq. 5.1.1, where $c_1 = 7.5 \text{ yr}^{-1}$, $p_1 = 1978$, $a_1 = 10$, $c_2 = 11.3 \text{ yr}^{-1}$, $p_2 = 1998.5$, $a_2 = 8$, with epochs I and II indicated.

A simulation is done including this time dependence of the calving parameter, of which the result is shown in Figure 5.1.4. Clearly, this simulates the observed length remarkably well. This justifies the use of a minimal model, in which the calving flux and surface mass balance describe the glaciers behaviour. An interesting question is, what the cause behind the increase of the calving flux during these two epochs could have been. When a linear relation between F and d is assumed and c is required to remain constant as well, then the water depth during the periods of rapid retreat should have increased by an exceptionally high factor. Assuming the width and ice thickness at the front to be constant would lead to 4.3 times deeper water during epoch I, and even 6.2 times deeper during epoch II, compared to a situation where the calving parameter has the constant value 1.65 yr^{-1} . These factors would lead to inconceivably deep water and do not correspond with observed water depths at all. The linear parametrization of the calving flux appears to be too rigorous here to explain the rapid retreat of Kronebreen.

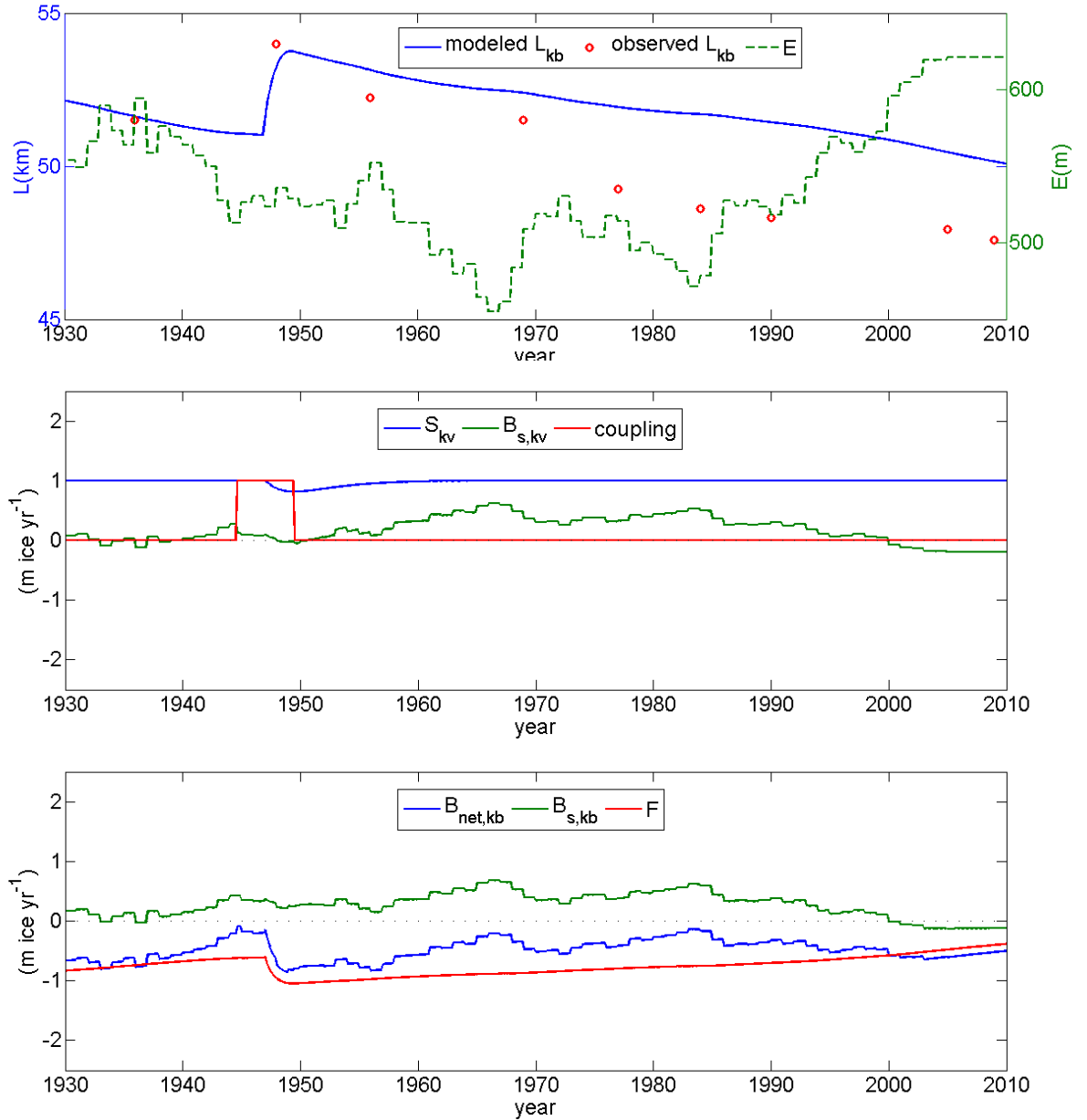


Figure 5.1.3: Close-up on period with front positions available. $E_{gem} = 507.5 \text{ m}$, $c = 1.65 \text{ yr}^{-1}$, $\beta = 0.0053 \text{ m w.e. m}^{-1}$, $\alpha_{m,kb} = 1.43$, $\alpha_{m,kv} = 2.27$.

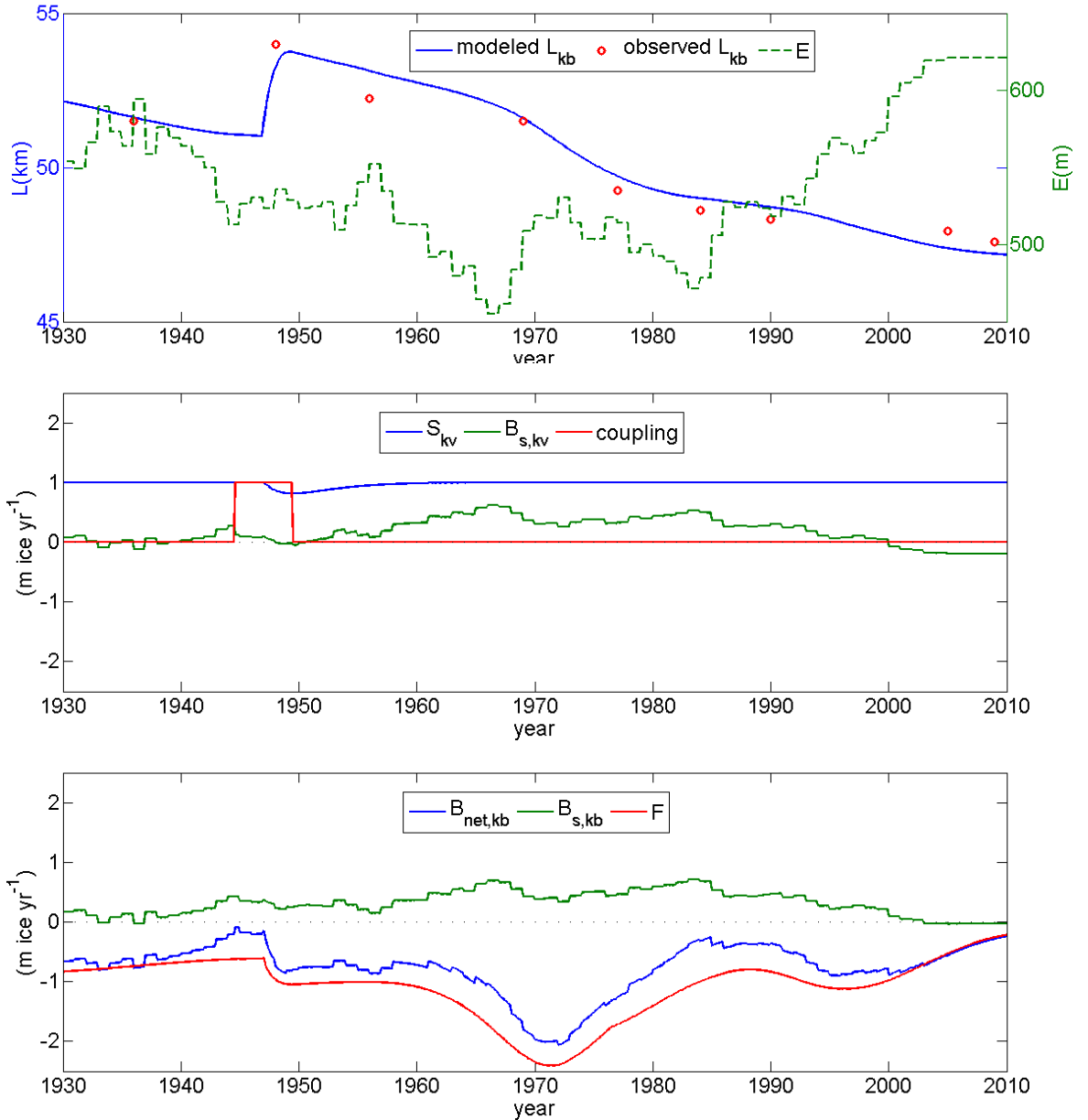


Figure 5.1.4: Data on calving flux included, $E_{gem} = 507.5$ m, c as in eq. 5.1.1, $\beta = 0.0053$ m w.e. m^{-1} , $\alpha_{m,kb} = 1.43$, $\alpha_{m,kv} = 2.27$.

5.2 Relation between glacier length equilibrium-line altitude

As noted in Section 4, the relation between E and L shown in Figure 4.0.6 is nonlinear. For some values of E , different steady states are possible, depending on whether the glacier is advancing or retreating. Two regions of hysteresis are visible, one visualizes the height-mass balance feedback and the other to the water depth-calving flux feedback caused by the overdeepening in the bed. The first is seen in the region near 1100m, because it takes a lower E to build up the glacier than to maintain it. This is a result of the higher elevation caused by a layer of ice, which leads to a higher surface mass balance with the same value of E . The glacier lengths between 44 and 48 km do not present stable equilibria, which is a consequence of the reversed bed slope and the fact that the calving flux increases with the water depth. When the glacier is in the upper branch, a small rise of the equilibrium-line altitude can cause to glacier to retreat rapidly. This is possible because a small rise of E will reduce the surface balance, so the net balance will be slightly negative, causing a retreat into deeper water. Then this will lead to an increasing calving flux which will reduce the net balance even more. With the current length of 47.6 km for Kronebreen, these feedback mechanisms will very likely cause a rapid retreat in near future.

5.3 Kronebreen and Kongsvegen in a warming climate

The IPCC makes its projections for different scenarios called Representative Concentration Pathways (RCPs) for greenhouse gas concentration. The most extreme ones are called RCP8.5 (which implies a radiative forcing of 8.5 W m^{-2} by 2100) and RCP2.6 (which shows a radiative forcing peak at 3 W m^{-2} and then declines to approximately 2.6 W m^{-2}). IPCC projections of temperature change and precipitation rate changes for the arctic are converted to a change in E using eq. 4.0.5. This results in a rise of 1.16 m yr^{-1} for the most persistent warming climate and 0.20 m yr^{-1} for the RCP2.6 from 2005 to 2100. The resulting volume for Kronebreen is modeled and shown with respect to the volume in 2005 in Figure 5.3.1. The scenario for which the climate conditions remain as they were in epoch II (1990–2007) until 2100, hence $c = 10.19 \text{ yr}^{-1}$ and $E = 572 \text{ m}$, is shown as a reference as well. It should be noted that in reality the equilibrium-line altitude will change more irregularly, and this will have some effect on the long-term behaviour of the glacier. Nonetheless, the scenario shown here provides a good first-order approximation of the expected retreat for Kronebreen.

Figure 5.3.1 shows an acceleration of the retreat of Kronebreen for RCP8.5 around the year 2090. The glacier seems to have passed a critical point here, since its volume starts to diverge from the other two scenarios. This happens at a length of $\sim 39 \text{ km}$, which could have been expected when taking Figure 4.0.6 into account again. Here it is clear that the steady state glacier passes a critical point around this length, from which retreat will suddenly get faster. The accelerating retreat leads to a decrease in volume of 41% with respect to 2005. For RCP2.6, Kronebreen will not pass this critical point before 2200 and will have lost only 24% of its volume. When climate conditions remain as they were on average during epoch II, Kronebreen reaches a steady state around 2160. By that time, it has lost 21% of its volume relative to 2005. This clearly shows that Kronebreen is currently out of balance with the existing climate.

The model describes Kongsvegen as a tributary glacier of Kronebreen, where the most important impact of Kongsvegen on Kronebreen is caused by its surge. Afterwards, Kongsvegen starts to retreat and the glaciers are decoupled. In the way the model is defined, all advance that Kongsvegen could have performed beyond 22.1 km is feeding Kronebreen. On the contrary, when dL/dt is negative, retreat starts immediately from 22.1 km. This results in a smaller glacier than Kongsvegen is in reality, since it actually lies parallel to Kronebreen instead of ending at 22.1 km. So Kongsvegens length in the model is not representative for its length as observed but for qualitative purposes it is possible to find out what Kongsvegens future looks like. As can be seen from Figure 5.3.2, both RCP2.6 and RCP8.5 will lead to a decrease in volume. Both RCPs lead to volume loss comparable to Kronebreen, respectively 22% and 44%. When climate conditions remain as they were on average in epoch II, Kongsvegen will gain 10% of its volume, without reaching its maximum value, but this is only in the case that no surges occur. Therefore, this scenario is not very likely and the shown projections can only be used to conclude that the model does not show a critical point for Kongsvegen.

6 Discussion and conclusion

In this study we have applied a minimal model to study the climate sensitivity of the Kongsvegen-Kronebreen system. We have demonstrated that only climate forcing is not enough to produce the observed behaviour. It is encouraging that forcing the model with measured calving flux magnitude, leads to a glacier evolution that is line with the observations. Therefore credible conclusions can be drawn on the present state of balance and the future of the system under conditions of climate change.

In parameterizing the calving flux, the linear relation between the calving flux and the water depth turned out to be too simple to explain the observed

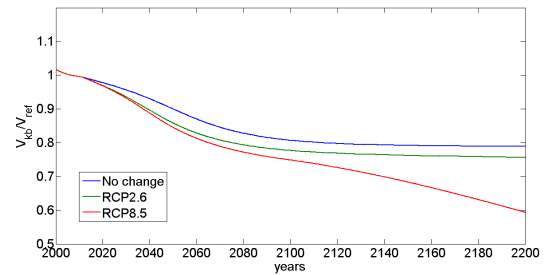


Figure 5.3.1: Projected ice volume Kronebreen, normalised to the volume in 2005.

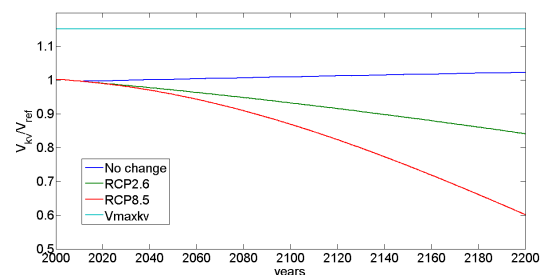


Figure 5.3.2: Projected ice volume Kongsvegen, normalised to the volume in 2005.

behaviour. Maybe the relation between water depth and calving flux is even stronger than linear, though even a quadratic dependence does not increase the calving flux enough to reach the estimated value. Other factors, as for example the ones named in the introduction, could be of influence. Besides that, the temperature of the water at the calving front which could vary in a different way than E and the depth of the crevasses near the glaciers front could be of impact on the calving flux. The characteristics of these crevasses could again be influenced by Kongsvegens surge. It appears here that the calving flux of a advancing glacier is smaller than the calving flux of a retreating glacier of the same length, since with the calving flux as observed for the two epochs is impossible to explain the build-up to its length in 1936. In this model, the mean ice thickness is parameterized in the same way for a retreating and an advancing glacier, which introduces another error. An explanation for the observed dynamics of tidewater calving glaciers was presented by A.S. Post in 1975,^[9] who suggested that the terminus of a tidewater glacier needed to be in shallow water to minimize its rate of calving. This indeed refers to a relation with the water depth, but he had an idea which explains the smaller calving flux for advancing glaciers. He suggested that a tidewater glacier builds a terminal moraine. In front of the moraine, the water depth could be hundreds of meters, but then the water depth at the front is shallow due to the moraine. If the glacier terminus is advancing, it does so by pushing the moraine further down-fjord. This involves erosion of the the moraine and deposition on the down-fjord side of the moraine. If the glacier loses contact with its moraine and retreats into deep water, its rate of calving will substantially increase. Including sediment dynamics will therefore lead to a more realistic representation of the calving flux. Besides that, Kronebreen is suggested to have surged in 1869 as well^[20], though it was not possible to get access to the article by Liestøl² which documents this surge.

Another limitation of the model is that it cannot present a joined calving front. As explained in Section 2.1, the portion of the calving front that Kronebreen occupies has varied over time. Just after the surge in 1948, Kongsvegen occupied almost half of the calving front whereas it has currently retreated onto land. Therefore, part of the retreat may also have been encouraged by Kronebreen taking over the southern part of the joint terminus area again after Kongsvegens surge. As the Kronebreen front widened, a larger part of the ice front consisted of Kronebreens fast-flowing ice, increasing the ice flux to the calving front. Keeping the width at the calving front constant for Kronebreen therefore introduces an error as well. Variations in the ice flux from Infantfonna will also have a slight impact on the calving rate as its basin constitutes over ten percent of the total area draining Kronebreen.^[20]

Despite its shortcomings, the minimal model seems to model the surface mass balance appropriately. Therefore, the fact that climate forcing alone cannot reproduce the glaciers behaviour is a robust result of this study. The limits of the minimal model seem to have been reached hereby. This emphasizes the importance of further study on modelling the calving flux, since there is still a lack of knowledge on the behaviour of calving glaciers.

While keeping the calving parameter constant, projections are made for the future volume of Kronebreen and Kongsvegen. With the smallest amount of global warming as expected by the IPCC, as in RCP2.6, both glaciers will lose over a fifth of their volume until 2200. Besides that, it is shown that Kronebreen is currently out of balance and will therefore also retreat without any further warming. It has been shown that a critical point is present around a length of 39 km for Kronebreen which will lead to an acceleration of the retreat. Under RCP8.5, the glacier will pass this critical point and shrink considerably to 59% of its volume in 2200, compared to 2005. Kronebreen will eventually disappear for this scenario but it will take about 700 years.

7 Acknowledgements

I would like to thank Hans Oerlemans for giving me the opportunity to use and explore your model, making me enthusiastic for this project and for sharing my enthusiasm throughout the semester. Thanks for the many hours you spent on guiding me in the right direction and teaching me everything on glaciers I needed to know. It was a great opportunity for me to see what it is like to be a researcher at the IMAU. Therefore I would like to thank the Ice and Climate group, since I enjoyed the weekly meeting and the diversity of the talks I attended. Thanks for coming to my talk as well, I really appreciate that I was taken seriously despite being only a bachelor student.

When starting this research, I had a hard time getting all programs installed and working on my computer. Thank you Jan-Willem for helping me, without your help it would have taken me much more time and frustrations. Of course thanks to all other students at the IMAU student room for your support and for convincing me to get a coffee when I needed a break.

²Liestøl O. 1988. The glaciers in the Kongsfjorden area, Spitsbergen. *Norsk Geogr. Tidsskr.* 42, 231-238.

References

- [1] Alean J. 2009. Glaciers online. <http://www.swisseduc.ch/glaciers/svalbard/kongsvegen/>
- [2] Baszczyk M., Jania J.A., Hagen J.O. 2009. Tidewater glaciers of Svalbard: recent changes and estimates of calving fluxes. *Polar Research* 30 (2), 85-142.
- [3] Budd W.F. 1975. A first simple model of periodically self-surging glaciers. *Journal of Glaciology* 14, 3-21.
- [4] Fowler A.C. 1987. A theory of glacier surges. *Journal of Geophysical Research (Solid Earth and Planets)* 92 (9), 9111-9120.
- [5] Hagen J.O., Sætrang A. 1991. Radio-echo soundings of sub-polar glaciers with low-frequency radar. *Polar Research* 9 (1), 99-107.
- [6] Kääb A., Lefauconnier B., Melvold K. 2005. Flow field of Kronebreen, Svalbard, using repeated Landsat 7 and ASTER data. *Annals of Glaciology* 42, 7-13.
- [7] Kamb B., Raymond C.F., Harrison W.D., Engelhardt H.F., Echelmeyer K.A., Humphrey N.F., Brugman M.M., Pfeffer T. 1985. Glacier surge mechanism, 1982-1983 surge of Variegated Glacier, Alaska. *Science* 227, 469-479.
- [8] Melvold K., Hagen J.O. 1998. Evolution of a surge-type glacier in its quiescent phase: Kongsvegen, Spitsbergen, 1964-95. *Journal of Glaciology* 44 (147),394-404.
- [9] Molnia B.F. 2007. Late nineteenth to early twenty-first century behavior of Alaskan glaciers as indicators of changing regional climate. *Global and Planetary Change* 56 (12), 23-56.
- [10] Norwegian Polar Institute, toposvalbard.npolar.no, visited on 28-11-2013.
- [11] Nuth C., Schuler T.V., Kohler J., Altena B., Hagen J.O. 2012. Estimating the long-term calving flux of Kronebreen, Svalbard, from geodetic elevation changes and mass-balance modelling. *Journal of Glaciology* 58 (207),119-133.
- [12] Oerlemans J. 2011. Minimal Glacier Models. Second edition. *Igitur, Utrecht University*, ISBN 978-90-6701-022-1.
- [13] Oerlemans J., Jania J.A., Kolondra L. 2011. Application of a minimal glacier model to Hansbreen, Svalbard. *The Cryosphere* 5, 1-11.
- [14] Østrem G., Brugman M. 1991. Glacier mass-balance measurements: a manual for field and office work. *NHRI Science Report No. 4*.
- [15] Van Pelt W.J.J., Oerlemans J., Reijmer C.H., Pohjola V.A., Pettersson R., Van Angelen J.H. 2012. Simulating melt, runoff and refreezing on Nordenskiöldbreen, Svalbard, using a coupled snow and energy balance model. *The Cryosphere* 6, 641-659.
- [16] Van Pelt W.J.J., Oerlemans J., Reijmer C.H., Pettersson R., Pohjola V.A., Divine D. 2013. An iterative inverse method to estimate basal topography and initialize ice flow models. *The Cryosphere* 7, 987-1006.
- [17] Post A.S. 1965. Alaskan glaciers: recent observations in respect to the earthquake advance theory. *Science* 148, 366-368
- [18] Post A.S. 1969. Distribution of surging glaciers in western North America. *Journal of Glaciology* 8 (53), 229-240
- [19] Russel I.C. 1897. Glaciers of North America. *Ginn and Co., Boston*, 210.
- [20] Sund M., Eiken T., Rolstad Denby C. 2011. Velocity structure, front position changes and calving of the tidewater glacier Kronebreen, Svalbard. *The Cryosphere Discuss.*, 5,41-73.
- [21] Sund M., Eiken T., Hagen J.O., and Kääb A. 2009. Svalbard surge dynamics derived from geometric changes. *Annals of Glaciology* 50(52), 50-60.
- [22] Trusel L.D., Powell R.D., Cumpston R.M., Brigham-Grette J. 2010. Modern glacial processes and potential future behaviour of Kronebreen and Kongsvegen polythermal tidewater glaciers, Kongsfjorden, Svalbard. *Geological Society, London, Special Publications* (344), 89-102.
- [23] Van der Veen C. J. 2002. Calving glaciers. *Progress in Physical Geography* 26(1), 96-122.

Appendices

A Derivations

A.1 Computation of mean bed elevation and slope

The mean bed elevation and mean slope are calculated from the bed profile parameterized as

$$b(x) = b_0 e^{-\frac{x}{x_2}} + b_1 e^{-\left(\frac{x-x_0}{x_l}\right)^2} - sx. \quad (\text{A.1.1})$$

Integration leads to

$$\begin{aligned} \bar{s} &= -\frac{1}{L} \int_0^L \frac{db}{dx} dx \\ &= -\frac{1}{L} [b(x)]_0^L \\ &= -\frac{1}{L} \left[b_0 e^{-\frac{x}{x_2}} + b_1 e^{-\left(\frac{x-x_0}{x_l}\right)^2} - sx \right]_0^L \\ &= \frac{b_0}{L} (1 - e^{-\frac{L}{x_2}}) + \frac{b_1}{L} \left(e^{-\left(\frac{x_0}{x_l}\right)^2} - e^{-\left(\frac{L-x_0}{x_l}\right)^2} \right) + s \end{aligned} \quad (\text{A.1.2})$$

For evaluating $\frac{d\bar{s}}{dL}$, this expression has to be differentiated with respect to L .

$$\begin{aligned} \frac{\partial \bar{s}}{\partial L} &= -\frac{b_0}{L^2} (1 - e^{-\frac{L}{x_2}}) + \frac{b_0}{Lx_2} e^{-\frac{L}{x_2}} + \frac{b_1}{L} e^{-\left(\frac{L-x_0}{x_l}\right)^2} 2 \frac{L-x_0}{x_l} \frac{1}{x_l} - \frac{b_1}{L^2} \left(e^{-\left(\frac{x_0}{x_l}\right)^2} - e^{-\left(\frac{L-x_0}{x_l}\right)^2} \right) \\ &= -\frac{b_0}{L^2} (1 - e^{-\frac{L}{x_2}}) + \frac{b_0}{Lx_2} e^{-\frac{L}{x_2}} + \frac{2b_1(L-x_0)}{x_l^2 L} e^{-\left(\frac{L-x_0}{x_l}\right)^2} - \frac{b_1}{L^2} \left(e^{-\left(\frac{x_0}{x_l}\right)^2} - e^{-\left(\frac{L-x_0}{x_l}\right)^2} \right) \end{aligned} \quad (\text{A.1.3})$$

The expression for \bar{b} requires some more cumbersome integration.

$$\bar{b} = \frac{1}{L} \int_0^L b(x) dx = \frac{1}{L} \int_0^L b_0 e^{-\frac{x}{x_2}} - sx dx + \frac{1}{L} \int_0^L b_1 e^{-\left(\frac{x-x_0}{x_l}\right)^2} dx$$

These two integrals will be evaluated separately. The first integral is easily evaluated:

$$\begin{aligned} \frac{1}{L} \int_0^L b_0 e^{-\frac{x}{x_2}} - sx dx &= \frac{1}{L} \left[-b_0 x_2 e^{-\frac{x}{x_2}} - \frac{s}{2} x^2 \right]_0^L \\ &= \frac{1}{L} \left(-b_0 x_2 (e^{-\frac{L}{x_2}} - 1) - \frac{s}{2} L^2 \right) \\ &= \frac{b_0 x_2}{L} (1 - e^{-\frac{L}{x_2}}) - \frac{sL}{2}. \end{aligned}$$

The second integral requires substitution of the variables $t = \frac{x-x_0}{x_l}$ and $s = -t$. For simplification of the expression, $x_a = \frac{L-x_0}{x_l}$ and $x_b = \frac{x_0}{x_l}$ will be substituted as well. Using $\frac{dx}{dt} = \frac{d}{dt}(tx_l + x_0) = x_l$ gives

$$\begin{aligned} \frac{1}{L} \int_0^L b_1 e^{-\left(\frac{x-x_0}{x_l}\right)^2} dx &= \frac{x_l b_1}{L} \int_{-x_b}^{x_a} e^{-t^2} dt \\ &= \frac{x_l b_1}{L} \left(\int_{-x_b}^0 e^{-t^2} dt + \int_0^{x_a} e^{-t^2} dt \right) \\ &= \frac{x_l b_1}{L} \left(\int_{x_b}^0 -e^{-s^2} ds + \int_0^{x_a} e^{-t^2} dt \right) \\ &= \frac{x_l b_1}{L} \left(\int_0^{x_b} e^{-s^2} ds + \int_0^{x_a} e^{-t^2} dt \right) \\ &= \frac{x_l b_1}{L} (\text{erf}(x_b) + \text{erf}(x_a)) \frac{\sqrt{\pi}}{2} \end{aligned}$$

Where $\text{erf}(x)$ is the error function, defined as

$$\text{erf}(x) = \frac{2}{\sqrt{\pi}} \int_0^x e^{-t^2} dt. \quad (\text{A.1.4})$$

Several approximations of the error functions are known, here we used

$$\text{erf}(x) \approx \text{sgn}(x) \sqrt{1 - e^{-x^2 \frac{4/\pi + ax^2}{1+ax^2}}}, \text{ where } a = \frac{8(\pi - 3)}{3\pi(4 - \pi)}. \quad (\text{A.1.5})$$

The sign function is used in this expression, which is defined as

$$\text{sgn}(x) = \frac{x}{|x|}, \text{ whenever } x \text{ is not equal to zero, then } \text{sgn}(0) = 0.$$

A.2 Evaluation of the continuity equation

From geometry we see $V = WH_mL$, so using eq. 3.2.1 this results in:

$$\begin{aligned} \frac{dV}{dt} &= \frac{d}{dt} (WH_mL) \\ &= W \left(L \frac{dH_m}{dt} + H_m \frac{dL}{dt} \right) \\ &= W \left(L \frac{d}{dt} \left[S(t) \frac{\alpha_m}{(1 + \nu \bar{s})} \sqrt{L} \right] + H_m \frac{dL}{dt} \right) \\ &= W \left(L \frac{\alpha_m}{(1 + \nu \bar{s})} \frac{d}{dt} \left[S(t) \sqrt{L} \right] + L \sqrt{L} S(t) \frac{d}{d\bar{s}} \left[\frac{\alpha_m}{(1 + \nu \bar{s})} \right] \frac{\partial \bar{s}}{\partial L} \frac{dL}{dt} + H_m \frac{dL}{dt} \right) \\ &= W \left(\frac{3}{2} H_m \frac{dL}{dt} + \frac{\alpha_m}{(1 + \nu \bar{s})} L^{3/2} \frac{dS}{dt} - L^{3/2} S(t) \frac{\alpha_m \nu}{(1 + \nu \bar{s})^2} \frac{\partial \bar{s}}{\partial L} \frac{dL}{dt} \right) \\ &= W \left(\frac{dL}{dt} \left[\frac{3}{2} H_m - \frac{L\nu H_m}{(1 + \nu \bar{s})} \frac{\partial \bar{s}}{\partial L} \right] + \frac{H_m L}{S(t)} \frac{dS}{dt} \right) \end{aligned} \quad (\text{A.2.1})$$

Possible changes in the total volume are assumed to be caused only by the surface mass balance B_s (eq. 3.0.3) and the calving flux F (eq. 3.1.1). Therefore,

$$\begin{aligned} W \left(\frac{dL}{dt} \left[\frac{3}{2} H_m - \frac{L\nu H_m}{(1 + \nu \bar{s})} \frac{\partial \bar{s}}{\partial L} \right] + \frac{H_m L}{S(t)} \frac{dS}{dt} \right) &= W\beta(\bar{b} + H_m - E)L - cdH_f W \text{ so} \\ W \frac{dL}{dt} \left[\frac{3}{2} H_m - \frac{L\nu H_m}{(1 + \nu \bar{s})} \frac{\partial \bar{s}}{\partial L} \right] &= W\beta(\bar{b} + H_m - E)L - cdH_f W - \frac{WH_m L}{S(t)} \frac{dS}{dt}. \end{aligned}$$

Hence

$$\begin{aligned} \frac{dL}{dt} &= \left(\beta(\bar{b} + H_m - E)L - cdH_f - \frac{H_m L}{S(t)} \frac{dS}{dt} \right) \left[\frac{3}{2} H_m - \frac{L\nu H_m}{(1 + \nu \bar{s})} \frac{\partial \bar{s}}{\partial L} \right]^{-1} \\ &= \left(\frac{B_s + F}{W} - \frac{H_m L}{S(t)} \frac{dS}{dt} \right) \left[\frac{3}{2} H_m - \frac{L\nu H_m}{(1 + \nu \bar{s})} \frac{\partial \bar{s}}{\partial L} \right]^{-1}, \end{aligned} \quad (\text{A.2.2})$$

when a single glacier is taken into account. Combining the two glaciers is done by solving

$$\frac{dV}{dt} = \frac{d}{dt} (W_{kb} H_{m,kb} L_{kb} + W_{kv} H_{m,kv} L_{kv}) = B_{s,kb} + F_{kb} + B_{s,kv}, \quad (\text{A.2.3})$$

and realizing that in the coupled case $\frac{dL_{kv}}{dt}$ is defined to be zero. Using the expressions as derived above, and writing all indexes kv and kb (only $F_{kb} = F$ since Kronebreen does all the calving and $S_{kv} = S$ since Kronebreen is assumed not to be a surging glacier) gives the combined expression:

$$\begin{aligned} W_{kb} \frac{d}{dt} (H_{m,kb} L_{kb}) + W_{kv} L_{kv} \frac{dH_{m,kv}}{dt} &= B_{s,kb} + F + B_{s,kv} \\ W_{kb} \frac{dL_{kb}}{dt} \left[\frac{3}{2} H_{m,kb} - \frac{L_{kb} \nu H_{m,kb}}{(1 + \nu \bar{s}_{kb})} \frac{\partial \bar{s}_{kb}}{\partial L_{kb}} \right] + W_{kv} \frac{H_{m,kv} L_{kv}}{S(t)} \frac{dS}{dt} &= B_{s,kb} + F + B_{s,kv} \\ W_{kb} \frac{dL_{kb}}{dt} \Psi_{kb} &= B_{s,kb} + F + B_{s,kv} - W_{kv} \frac{H_{m,kv} L_{kv}}{S(t)} \frac{dS}{dt} \end{aligned}$$

$$\text{so } \frac{dL_{kb}}{dt} = \left(B_{s,kb} + F + B_{s,kv} - W_{kv} \frac{H_{m,kv} L_{kv}}{S(t)} \frac{dS}{dt} \right) [W_{kb} \Psi_{kb}]^{-1} \quad (\text{A.2.4})$$

Note that all dependence on width vanishes when $W_{kv} = W_{kb}$ is assumed such that

$$\begin{aligned} \frac{dL_{kb}}{dt} &= \left(\frac{B_{s,kb} + F + B_{s,kv}}{W_{kb}} - \frac{H_{m,kv} L_{kv}}{S(t)} \frac{dS}{dt} \right) \Psi_{kb}^{-1} \\ &= \left(\beta(\bar{b}_{kb} + H_{m,kb} - E_{kb})L_{kb} - cdH_f + \beta(\bar{b}_{kv} + H_{m,kv} - E_{kv})L_{kv} - \frac{H_{m,kv} L_{kv}}{S(t)} \frac{dS}{dt} \right) \Psi_{kb}^{-1} \end{aligned} \quad (\text{A.2.5})$$

B Fortran code

```
program twoglacier
implicit none
  real b0kv , x1kv , x0kv , x2kv , b1kv , skv , betakv , Lkv , sgemkv , Bskv
  real Hmkv , dsdLkv , bmkv , dLdtkv , bnetkv , Lkmkv , PSIkV , Bsnkv , Lmaxkv
  real Snkv , alfamkv , nu , pi , delta , Eref , a , E , xkm , x , bedm , F , c , Hf , kappa
  real t0 , ts , q0 , Bsover , Lover , alfamkb , Ekv , b0kb , x1kb , x0kb , x2kb , b1kb
  real skb , betakb , Lkb , sgemkb , Bskb , Hmkb , dsdLkb , bmkb , dLdtkb , bnetkb
  real Lkmkb , PSIkB , Bsnkb , Fnkb , xakv , xbkv , xakb , xkb , hulp1kv , hulp2kv
  real hulp1kb , hulp2kb , erfLkv , erf0kv , erfLkb , erf0kb , dat(1422) , dE(711)
  real tijd , koppel , c0 , c1 , c2 , p1 , p2 , a1 , a2 , Vrefkv , Vkv , Vrefkb , Vkb
  real dt , timemax , time , grens1 , grens2 , Vmaxkv , dsim
  integer i , itime

  open( unit=15, file='CAL-EVO2kv.txt ' )
  open( unit=16, file='CAL-EVO2kb.txt ' )
  open( unit=2, file='CAL-PRO2kb.txt ' )
  open( unit=3, file='CAL-PRO2kv.txt ' )
  open( unit=4, file='C:\Users\Eef\SvalbardClimateData3.txt ' )

  read (4,*) dat
  do i=1,711
    dE(i)=dat(2*i)
  end do

  write (15,109)
  write (16,110)
  write (2,108)
  write (3,108)

  pi=2*acos(0.0)
  a=8*(pi-3)/(3*pi*(4-pi))
  delta = 0.9998/0.9167
  nu=10.
  Eref=501.+88.
  dt = 0.125
  time = 0.875
  timemax = 2200

  b0kv = 461.5
  b1kv = 146.8
  skv = 0.0092
  x1kv = -7088
  x0kv = 25421
  x2kv = 12303
  betakv=0.0053
  alfamkv=2.27
  Lkv=1.
  Lmaxkv=22100.

  b0kb =1089.
  x2kb =25800
  skb =0.00582
  b1kb =71.0
  x0kb =47800
  x1kb =2550
  betakb=0.0053
```

```

alfamkb=1.43
c=1.3
kappa=0.4
Lkb=1.

do i=1,500
x=(i-1)*100.
xkm=x/1000.
bedm=bedkv(x)
write (3,100) xkm,bedm
end do

do i=1,700
x=(i-1)*100.
xkm=x/1000.
bedm=bedkb(x)
write (2,100) xkm,bedm
end do

t0=1947
ts=2.5
q0=0.2

c0 = 1.65
c1 = 7.5
c2 = 11.3
p1 =1978
p2 =1998.5
a1 =10
a2 =8

Vrefkb=47360*251.807
Vrefkv=20324*262.577
Vmaxkv=22100*278.238

99 continue
time=time+dt
itime=int(time)

c = calving(time)
grens1=1299.875
grens2=2010.875
if (time.lt.1300) E=Eref-150.+(time-299)*150/1000.
if (time.gt.grens1.and.time.lt.2011) E=Eref+dE(itime-1299)
if (time.gt.grens2) E=572.4 !E+1.16*dt
if (time.gt.grens2) c=10.19

Ekv=E-200

xakv=(Lkv-x0kv)/xlkv
xbkv=x0kv/xlkv
sgemkv=b0kv*(1.-exp(-Lkv/x2kv))/Lkv+skv-b1kv/Lkv*exp(-xakv**2)
sgemkv=sgemkv+b1kv/Lkv*exp(-xbkv**2)
hulp1kv=-xakv**2*(4/pi+a*xakv**2)/(1+a*xakv**2)
erfLkv=sqrt(1-exp(hulp1kv))
if (Lkv.lt.x0kv) erfLkv=-erfLkv
hulp2kv=-xbkv**2*(4/pi+a*xbkv**2)/(1+a*xbkv**2)
erf0kv=sqrt(1-exp(hulp2kv))

```

```

bmkv=x2kv*b0kv/Lkv*(1-exp(-Lkv/x2kv))
bmkv=bmkv-0.5*skv*Lkv+b1kv*xlkv*sqrt(pi)/2./Lkv*(erfLkv+erf0kv)
Hmkv=alfamkv/(1+nu*sgemkv)*sqrt(Lkv)*surge(time)
Bskv=betakv*(Hmkv+bmkv-Ekv)*Lkv
dsdLkv=b0kv*(1-exp(-Lkv/x2kv))/Lkv**2+b0kv/x2kv/Lkv*exp(-Lkv/x2kv)
dsdLkv=dsdLkv+2*b1kv*(Lkv-x0kv)/(xlkv**2*Lkv)*exp(-xakv**2)
dsdLkv=dsdLkv-b1kv/(Lkv**2)*(exp(-xbkv**2)-exp(-xakv**2))
PSlkv=3/2.*Hmkv-alfamkv*nu/(1+nu*sgemkv)**2*Lkv**1.5*dsdLkv*surge(time)

xakb=(Lkb-x0kb)/xlkb
xbkb=x0kb/xlkb
sgemkb=b0kb*(1-exp(-Lkb/x2kb))/Lkb+skb
sgemkb=sgemkb-b1kb/Lkb*exp(-xakb**2)+b1kb/Lkb*exp(-xbkb**2)
hulp1kb=xakb**2*(4/pi+a*xakb**2)/(1+a*xakb**2)
erfLkb=sqrt(1-exp(hulp1kb))
if (Lkb.lt.x0kb) erfLkb=-erfLkb
hulp2kb=xbkb**2*(4/pi+a*xbkb**2)/(1+a*xbkb**2)
erf0kb=sqrt(1-exp(hulp2kb))
bmkb=x2kb*b0kb/Lkb*(1-exp(-Lkb/x2kb))
bmkb=bmkb-0.5*skb*Lkb+b1kb*xlkb*sqrt(pi)/2./Lkb*(erfLkb+erf0kb)
Hmkb=alfamkb/(1+nu*sgemkb)*sqrt(Lkb)
Bskb=betakb*(Hmkb+bmkb-E)*Lkb
Hf = max(kappa*Hmkb,-delta*bedkb(Lkb))
F=c*bedkb(Lkb)*Hf
if (bedkb(Lkb).gt.0) F=0
dsdLkb=b0kb*(1-exp(-Lkb/x2kb))/Lkb**2+b0kb/x2kb/Lkb*exp(-Lkb/x2kb)
dsdLkb=dsdLkb+2*b1kb*(Lkb-x0kb)/(xlkb**2*Lkb)*exp(-xakb**2)
dsdLkb=dsdLkb-b1kb/(Lkb**2)*(exp(-xbkb**2)-exp(-xakb**2))
PSlkb=3/2.*Hmkb-alfamkb*nu/(1+nu*sgemkb)**2*Lkb**1.5*dsdLkb

dLdtkv=(Bskv-alfamkv/(1+nu*sgemkv)*Lkv**1.5*dsdt(time))/PSlkv
if (Lkv.gt.(Lmaxkv-1.).and.dLdtkv.gt.0.) then
dLdtkv=0.
dLdtkb=(Bskb+F+Bskv-alfamkv/(1+nu*sgemkv)*Lkv**1.5*dsdt(time))
dLdtkb=dLdtkb/PSlkb
koppel=1
Lkv=Lkv+dt*dLdtkv
if (Lkv.gt.(Lmaxkv-1.)) Lkv=Lmaxkv
Lkmkv=Lkv/1000.
bnetkv=(Bskv-alfamkv/(1+nu*sgemkv)*Lkv**1.5*dsdt(time))/Lkb
Bsnkv = Bskv/Lkb
Snkv = -alfamkv/(1+nu*sgemkv)*Lkv**1.5*dsdt(time)/Lkb
Lkb=Lkb+dt*dLdtkb
if (Lkb.lt.1.) Lkb=1.
Lkmkb=Lkb/1000.
bnetkb=(Bskb+F+Bskv)/Lkb
Bsnkb = Bskb/Lkb
Fnkb = F/Lkb

else
dLdtkb=(Bskb+F)/PSlkb
koppel=0
Lkv=Lkv+dt*dLdtkv
Lkb=Lkb+dt*dLdtkb
if (Lkv.gt.Lmaxkv) then
Lover=Lkv-Lmaxkv
Lkv=Lmaxkv
Bsover=Lover*PSlkv
dLdtkb=Bsover/PSlkb

```



```

Lkb=Lkb+dt*dLdtkb
koppel=1
bnetkb=(Bskb+F+Bsover)/Lkb
goto 70
    else
        bnetkb=(Bskb+F)/Lkb
        if (Lkv.lt.1.) Lkv=1.
        Lkmkv=Lkv/1000.
        bnetkv=(Bskv-alfamkv/(1+nu*sgemkv)*Lkv**1.5*dstd(time))/Lkv
        Bsnkv = Bskv/Lkv
        Snkv = -alfamkv/(1+nu*sgemkv)*Lkv**1.5*dstd(time)/Lkb
        if (Lkb.lt.1.) Lkb=1.
        Lkmkb=Lkb/1000.
        Bsnkb = Bskb/Lkb
        Fnkb = F/Lkb
        if(time.gt.3009.and.time.lt.3011) print *,Lkmkb
    end if
end if

Vkb = Hmkb*Lkb
Vkv = Hmkv*Lkv
tijd = time
if (surge(time).lt.0) print *, "Hm<0. Program aborted."
if (surge(time).lt.0) goto 80

!write (15,100) tijd , Lkmkv,bnetkv,Ekv,Hmkv,Bsnkv,Snkv, koppel
!write (16,100) tijd , Lkmkb,bnetkb,E,Hmkb,Bsnkb,Fnkb,c, bedkb(Lkb),dsim
write (15,100) tijd , Lkmkv,Ekv, Vkv/Vrefkv,Vmaxkv/Vrefkv,Hmkv
write (16,100) tijd , Lkmkb, E, Vkb/Vrefkb

if (time.lt.timemax) goto 99

80 continue

100 format (1x,10F11.3)

108 format (1x,"xkmbed")
109 format (1x,"timeLbnetE HmBsSterminbnetkoppelvoorKongsvegen")
110 format (1x,"timeLbnetE HmBsFvoorKronebreen")

contains

function bedkv(x)
    real :: x,bedkv
    bedkv=b0kv*exp(-x/x2kv)-skv*x + b1kv*exp(-((x-x0kv)/xlkv)**2)
end function bedkv

function bedkb(x)
    real :: x,bedkb
    bedkb=b0kb*exp(-x/x2kb)-skb*x + b1kb*exp(-((x-x0kb)/xlkb)**2)
end function bedkb

function calving(w)
    real :: calving,w
    calving = c0 + c1*exp(-((w - p1)/a1)**2) + c2*exp(-((w - p2)/a2)**2)
end function calving

function surge(w)

```

```

    real :: w,w2, surge , t02
    if (w.lt.t0) then
        surge = 1
    else
        w2 = w-1947
        !w2 = mod(w2,150.)
        t02 = 0
        surge = 1.-q0*(w2-t02)*exp(-(w2-t02)/ts)
    end if
    !if (w.gt.2490) surge = 1
end function surge

function dsdt(w)
    real :: w,w2, dsdt , t02
    if (w.lt.t0) then
        dsdt = 0
    else
        w2=w-1947
        !w2= mod(w2,150.)
        t02 = 0
        dsdt = q0*((w2-t02)/ts -1)*exp(-(w2-t02)/ts)
    end if
    !if (w.gt.2490) dsdt = 0
end function dsdt

end program twoglacier

```